

# Thermally Responsive Poly[*N*-isopropylacrylamide-*co*-2-hydroxyethylacrylate] Colloidal Crystals Included in $\beta$ -Cyclodextrin for Controlled Drug Delivery

Anu Stella Mathews, Won-Jei Cho, Il Kim, Chang-Sik Ha

Department of Polymer Science and Engineering, Pusan National University, Busan 609-735, Republic of Korea

Received 24 March 2008; accepted 23 May 2008

DOI 10.1002/app.30164

Published online 17 April 2009 in Wiley InterScience (www.interscience.wiley.com).

**ABSTRACT:** Novel temperature-sensitive poly[*N*-isopropylacrylamide-*co*-2-hydroxyethylacrylate] [P(NIPAAm-HEAc)] colloidal crystals containing  $\beta$ -cyclodextrin ( $\beta$ -CD) were prepared. These reversibly tunable supramolecular inclusion complexes display brilliant colors, due to the self-assembly of several structured nanoparticles to form crystal structures. The hydrogels displayed rainbow colors upon the variation of the  $\beta$ -CD concentration and can be made either visible or invisible by simply changing the temperature. The inclusion complexes were characterized using NMR spectroscopy, laser light scattering, UV-visible spectroscopy, and viscometer measurements. Compared with the conventional poly(*N*-isopropylacrylamide) gel, the  $\beta$ -CD-incorporated hydrogels in aqueous solution showed a lower critical solution temperature of about 57°C, which can be attributed to the hydrogen bonding

between P(NIPAAm-HEAc) included in  $\beta$ -CD and water, which is enhanced by the hydrophilic groups of  $\beta$ -CD. The use of these materials as drug carriers was also evaluated by making use of their thermo-responsive behavior. The release time of a model drug, 5-fluorouracil (5-FU), from the novel inclusion complexes was prolonged in comparison to that from P(NIPAAm-HEAc) without  $\beta$ -CD. The significance of the present drug delivery system is the mixing of the gel and drug without any chemical reaction at room temperature, resulting in a gelled drug depot for slow and controlled release. © 2009 Wiley Periodicals, Inc. *J Appl Polym Sci* 113: 1680–1689, 2009

**Key words:** *N*-isopropylacrylamide; cyclodextrin inclusion complex; thermo-sensitivity; colloidal crystal; drug delivery

## INTRODUCTION

Polymeric gels represent a class of three-dimensional macromolecular networks containing a large fraction of solvent within their structure. A unique physical property of some of these gels is their reversible response to external stimuli such as temperature,<sup>1</sup> pH,<sup>2</sup> electric fields,<sup>3</sup> and solvents.<sup>4</sup> These materials, especially “intelligent” aqueous polymer systems named hydrogels,<sup>5</sup> find immense potential applications in medicine, biotechnology, industry, and in environmental problems.<sup>6–10</sup> Among the various environmentally responsive hydrogels, thermally responsive ones based on poly(*N*-isopropylacrylamide) (PNIPAAm) are of particular interest to researchers,

due to their dramatic and reversible transition behavior.<sup>11</sup> PNIPAAm homopolymer exhibits a lower critical solution temperature (LCST) of around 33°C in aqueous solution, and its hydrogel swells and shrinks in water below and above this temperature. An important and utile feature of PNIPAAm is the possibility of tailoring this coil-globule transition by incorporating comonomers<sup>12</sup> into the polymer and by adding cosolvents,<sup>13</sup> simple salts,<sup>14</sup> or surfactants<sup>15</sup> to the polymer solution. Chemical modifications have been carried out by incorporating another functional component into the PNIPAAm chain to extend its range of applications. These hydrogels can be prepared by copolymerizing two different monomers,<sup>16</sup> by forming interpenetrating polymer networks<sup>17</sup> or by creating networks with microporous structures.<sup>18</sup> The hydrogels can be made in bulk or in nano or micro particle form. The bulk-gels are easy to handle but usually have very slow swelling rates. Gel nanoparticles react quickly to an external stimulus but may be too small for practical applications. Recently, Hu and Gao<sup>19</sup> stabilized PNIPAAm nanoparticles in bulk forms by covalently bonding the self-assembled nanoparticles to form a network. Thus, stabilized nanoparticle networks offer new arenas of research, due to the merits arising from

Correspondence to: C.-S. Ha (cscha@pusan.ac.kr).

Contract grant sponsor: Ministry of Science and Technology (MOST) [Korea Science and Engineering Foundation (KOSEF) through the National Research Laboratory Program]; contract grant number: M10300000369-06J0000-36910.

Contract grant sponsor: SRC/ERC Program of MOST/KOSEF; contract grant number: R11-2000-070-080020.

Contract grant sponsor: Brain Korea 21 Project.

the quick response of the nanoparticles to stimuli, together with their structural and mechanical stability.

Supramolecular architectures of stabilized polymer chains threaded through cyclic components prepared as composite host/guest polymeric assemblies have recently emerged as a fascinating new field of macromolecular research. Cyclodextrin (CD), which consists of truncated cone-shaped oligosaccharides derived from starch, is one of the most popular host molecules employed in the construction of molecular assemblies. CDs are a family of cyclic oligosaccharides,  $\alpha$ ,  $\beta$ , and  $\gamma$ , comprising six to eight glucose units linked through  $\alpha(1\rightarrow4)$ -linkages, respectively.<sup>20</sup> A CD molecule has a hydrophobic internal cavity that enables it to include guest polymer molecules, thus forming supramolecular inclusion complexes stabilized by noncovalent interactions originating from the threading of the CD molecules through the polymer chains.<sup>21,22</sup> This complex formation leads to widespread applications in pharmaceutical chemistry, food technology, analytical chemistry, chemical synthesis, and food catalysis.<sup>23,24</sup>

In this study, the polymerization of PNIPAAm was performed in the presence of  $\beta$ -CD. We chose this particular method because it was expected to enhance the biocompatibility and stability of the PNIPAAm nanoparticles without covalently bonding them. The self-assembly of the cyclodextrin encapsulating the particles to obtain colloidal crystals allows us to obtain useful functionalities, originating not only from the colloidal particles themselves, but also from their long-range ordering.<sup>25</sup> Moreover, the effect of the  $\beta$ -CD concentration on the LCST behavior and the drug delivery behavior of the polymers using the model drug 5-fluorouracil (5-FU) is also focused on. 5-FU, a fluorinated pyrimidine, is a key anti-colorectal cancer drug that affects the synthesis and repair of DNA and RNA processing in cancer cells and has been used as an antitumor drug. The specificity of delivery using nanoparticles was initially a coincidental property; however, active targeting has now become a central concept in therapeutical research,<sup>26,27</sup> which motivated us to evaluate the release profile of the nanoparticles included in the  $\beta$ -CD cavities. A drug molecule included inside the cavity of CD could be easily dissociated upon dilution or replaced by a suitable guest.<sup>28</sup> Eventually, the incorporation of CDs into polymeric drug delivery systems could change the drug-polymeric interaction.<sup>29</sup> As a result, the mechanisms of drug release can be modified. Therefore, we also compared the properties and release studies of the CD containing colloidal crystals with our previously reported<sup>9</sup> PNIPAAm nanoparticles without CD. The novelty of our work lies in the stabilization of the hydrogel nanoparticles by successfully includ-

ing them in the  $\beta$ -CD cavities, the formation of rainbow colors, and colloidal crystals, depending on the cyclodextrin concentration and thermo-responsive controlled drug release of the resulting samples. Therefore our present investigation describes the manufacturing process, including the synthesis of poly[*N*-isopropyl acrylamide-*co*-2-hydroxyethylacrylate] [P(NIPAAm-HEAc)] hydrogel nanoparticles containing  $\beta$ -CD, the self-assembly of these particles to form colloidal crystals and the application of these particles as a promising candidate for controlled drug delivery applications.

## EXPERIMENTAL

### Materials

NIPAm was recrystallized from a benzene/*n*-hexane mixture. *N,N'*-Methylene-bis-acrylamide (MBS) and potassium persulfate (KPS) were purified by recrystallizing them three times from methanol.  $\beta$ -CD, 2-hydroxymethylacrylate (HEAc), sodium dodecyl sulfate (SDS), and divinyl sulfone (DVS) were used as obtained from Sigma-Aldrich Korea (Seoul, Korea) without any further purification. 5-FU was purified by recrystallizing from ethanol. All reactions were performed under a purified nitrogen atmosphere using standard Schlenk techniques.

### Sample preparation

The precipitation polymerization of NIPAAm in the presence of  $\beta$ -CD was carried out in a flask equipped with a mechanical stirrer and nitrogen feed. NIPAm, MBS, and SDS were dissolved in deionized water (DW), under continuous stirring.  $N_2$  gas was bubbled into the solution for 1 h. HEAc was added dropwise, followed by  $\beta$ -CD, before placing the flask into a 70°C hot bath. After heating the solution to 70°C under nitrogen for 40 min, KPS was added to initiate polymerization. The reaction was carried out at 70°C  $\pm$  1°C under an  $N_2$  atmosphere for 5 h to ensure that all of the monomer reacted. After cooling down to room temperature, the resulting P(NIPAAm-HEAc) nanoparticles dispersed in  $\beta$ -CD were purified via dialysis (MEMBRA-CEL MD34-7, molecular weight cutoff: 7000) by changing the stirring water outside the dialysis tube twice a day for 2 weeks, at room temperature. The resultant dispersion was further purified by ultracentrifugation to remove all unreacted chemicals and small molecules. The concentration of the dialyzed dispersion was calculated from the weight difference of the solution before and after drying at 120°C. Table I shows the feed ratios for the polymerization.

Different concentrations of the centrifuged particle suspensions were prepared in deionized water. The

TABLE I  
The Feed Ratio of P(NIPAAm-HEAc)/ $\beta$ -CD Complexes Prepared by Radical Polymerization

Sample	NIPAAm (mmol)	$\beta$ -CD (mmol)	HEAc (mmol)	MBS (mmol)	SDS (mmol)	KPS (mmol)	DW (mL)
1	3.35	0	0.342	0.05	0.04	0.06	26
2	3.35	0.17	0.342	0.05	0.04	0.06	26
3	3.35	0.34	0.342	0.05	0.04	0.06	26
4	3.35	0.51	0.342	0.05	0.04	0.06	26
5	3.35	0.67	0.342	0.05	0.04	0.06	26

concentration range was adjusted from 1.6 to 3 wt %. The particles in water were heated above their LCST by sonication, cooled below 25°C, and finally incubated for several days. The samples kept static for several days gave beautiful colloidal crystals arising from the self-assembly of the P(NIPAAm-HEAc) nanoparticles in  $\beta$ -CD.

### <sup>1</sup>H-NMR spectroscopy

The <sup>1</sup>H-NMR spectra were obtained at 300 MHz at an ambient temperature of 24°C  $\pm$  1°C on a Varian Unity Plus-300 NMR spectrometer, and the chemical shifts are reported in ppm units with tetramethylsilane as the internal standard.

### Laser light scattering

The average radii and their distribution for the P(NIPAAm-HEAc) and P(NIPAAm-HEAc)/ $\beta$ -CD nanoparticles in  $\beta$ -CD were observed using an electrophoretic light scattering (LLS) instrument with an He-Ne laser source (Photal ELS-8000, Otsuka Electronic, Osaka, Japan). The LLS experiments were performed at a scattering angle of 90°. The available detection size range is from 2 nm to 3  $\mu$ m.

### UV-visible spectroscopy measurements

The environmentally induced color change of the nonbonded and bonded hydrogels was measured using a UV-visible spectrometer (SHIMADZU 1650PC). The spectra of the hydrogels were recorded at different temperatures and different concentrations of  $\beta$ -CD.

### Rheological measurements

The viscosities of the aqueous dispersion were measured using a Brookfield viscometer. The temperature was adjusted by a water circulation bath. The measuring unit was equipped with a solvent trap to prevent water evaporation when the experiments were performed at high temperatures of up to 40°C.

### 5-FU loading and release

The samples were thoroughly washed using deionized water and perfectly dried before loading 5-FU. A predefined amount of the perfectly dried P(NIPAAm-HEAc)/ $\beta$ -CD particles was then allowed to swell in a given amount of 5-FU dissolved in 10 mL of buffer solution at 27°C. The amount of drug absorbed into the matrix was monitored using a UV-visible spectrometer at regular intervals of time until a constant value was reached.

Each loaded hydrogel was then rinsed with water and directly immersed into vials containing 10 mL pH 7 buffer solution placed in water baths at different temperatures to evaluate the temperature-sensitive release behavior. The amount of drug absorbed into the hydrogel matrix and released was also monitored using a UV-visible spectrometer at regular intervals of time until a constant value was reached. The release profiles between 10 and 70% release were characterized by fitting the following equation by nonlinear regression.<sup>7</sup>

$$M_t/M_\infty = kt^n, \quad (1)$$

where  $M_t/M_\infty$  is the fraction of the drug released at time  $t$ . All of the release measurements were carried out in duplicate for each hydrogel and the average values were plotted.

## RESULTS

### Structural confirmation

Figure 1 shows the <sup>1</sup>H-NMR spectra of P(NIPAAm-HEAc) (Sample 1) and P(NIPAAm-HEAc)/ $\beta$ -CD (Sample 3). The peaks corresponding to  $-\text{CH}_3$  (1.20 ppm),  $-\text{CH}$  (3.92 ppm),  $-\text{OH}$  (broad peak at 2.00 ppm) and  $-\text{NH}$  (broad peak at 7.39 ppm) were observed for Sample 1. For all of the other compounds, the characteristic peaks of  $\beta$ -CD, whose intensities varied according to the concentration, were seen together with the P(NIPAAm-HEAc) peaks, thus confirming the presence of  $\beta$ -CD in all of the hydrogels formed. The incorporation of  $\beta$ -CD caused the shift of the characteristic peaks of P(NIPAAm-HEAc) to 1.00 ppm ( $-\text{CH}_3$ ) and 3.84 ppm ( $-\text{CH}$ ), whereas the peaks of  $\beta$ -CD in the inclusion complex did not change in comparison

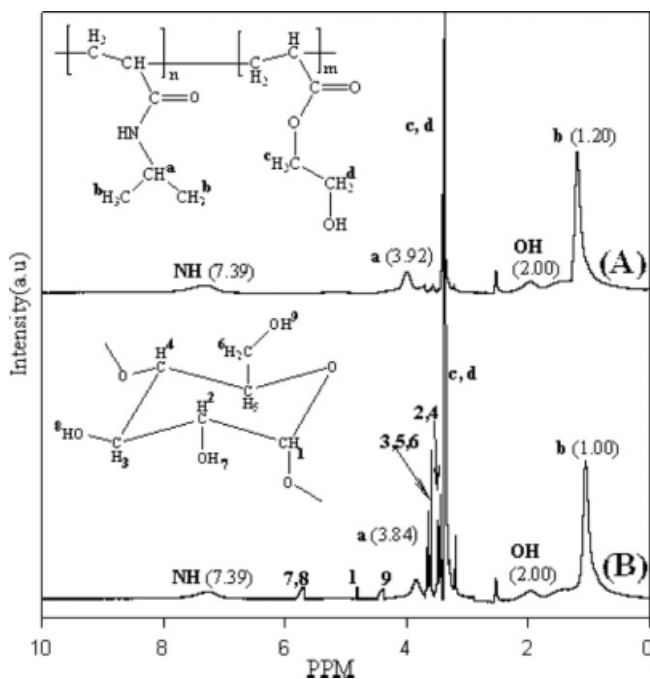


**Figure 1**  $^1\text{H}$ -NMR spectra of (A) Sample 1 [P(NIPAAm-HEAc)] and (B) Sample 3 [P(NIPAAm-HEAc)/ $\beta$ -CD] inclusion complex.

with those of  $\beta$ -CD itself. These up field shifts of the P(NIPAAm-HEAc) peaks in the complex suggest that the protons of the polymer chain are included in CD and shielded by it.<sup>30</sup>

### Rainbow colors and colloidal crystals

The visual appearance of the P(NIPAAm-HEAc) nanoparticles in  $\beta$ -CD is shown in Figure 2. The interesting rainbow colors displayed by the samples may be due to light interference from the closely packed nanoparticles.<sup>31</sup> The color changed from deep red to blue according to the concentration of  $\beta$ -CD for 6 wt % of the polymer in water. For higher concentrations of  $\beta$ -CD (i.e., Sample 5), the gel exhibited a deep red color. This can be attributed to the increase in the particle size. As the concentration of  $\beta$ -CD decreased, the color shifted to lower wavelength regions, due to the decrease in the particle size resulting from the reduction in the amount of polymer incorporated in the CD cavities. For the lower concentrations (below 4% polymer in water) of Samples 1, 2, and 3, a crystal phase occurred, as shown in Figure 2(B), indicating that the particles self-assembled to form a macrocrystal phase of long-range order. When the concentration of the polymer in water was above 4 wt %, the crystals were too small to be observed and the particles self-assembled into a glass phase of short-range order. As the concentration of  $\beta$ -CD increased, the crystal grain size decreased and, for Samples 4 and 5, the crystals

were too small to be observed, due to the short-range ordered glass phase of the self-assembled nanoparticles. This trend is similar to that previously reported for covalently bonded PNIPAAm nanoparticles.<sup>32</sup>

To quantify these observations, we measured the turbidity of the sample dispersions as a function of wavelength using a spectrophotometer, as shown in Figure 3. This method is similar to the techniques used to study colloidal particles in previous literature.<sup>19,33</sup> Corresponding to the appearance of the colors, a shoulder-shaped increase was seen, which shifted to higher wavelengths as the CD concentration increased. The color of the samples can thus be shifted by varying either the concentration or the particle size,<sup>19</sup> due to the change in the interparticle distance ( $d$ ), which is influenced by the incorporation of CD. According to previous studies,<sup>19,33</sup> the lattices' dimensions of colloidal crystals usually exceed 100 nm, causing Bragg diffraction of visible light, which is given by the well-known Bragg's equation:  $n\lambda = 2d \sin \theta$ , where  $\lambda$  is the diffracted wavelength,  $d$  is the interparticle distance,  $n$  is the refractive index of the dispersion, and  $\theta$  is the Bragg angle between the incident light beam and the  $d$  planes.<sup>33</sup> If we take  $\lambda_c$  as the transition wavelength at the position of the half height of the shoulder, for poly-crystals, it is reported that the Bragg diffraction

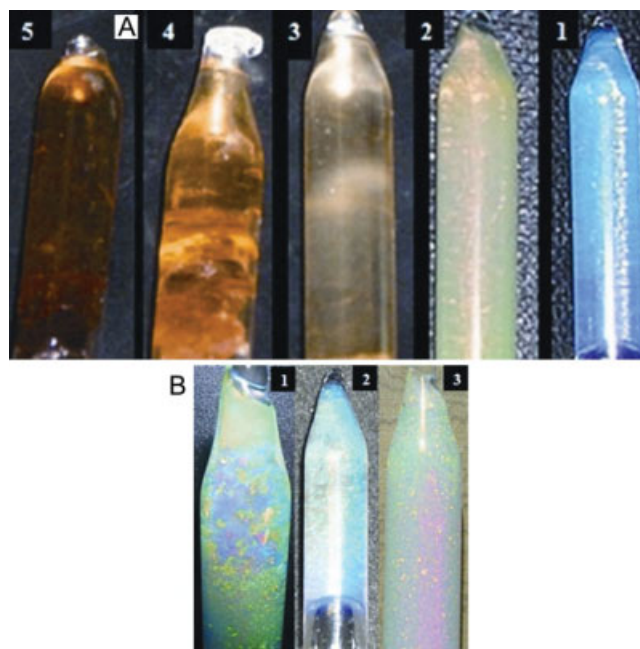


**Figure 2** (A)  $\beta$ -CD concentration-dependent color change of P(NIPAAm-HEAc) nanoparticles with particle weight percentage of 6.0%. (B) Highlights of crystal phase obtained for Samples 1, 2, and 3 at 3, 2.5, and 2% of polymer dispersion in water, respectively. [Color figure can be viewed in the online issue, which is available at [www.interscience.wiley.com](http://www.interscience.wiley.com).]

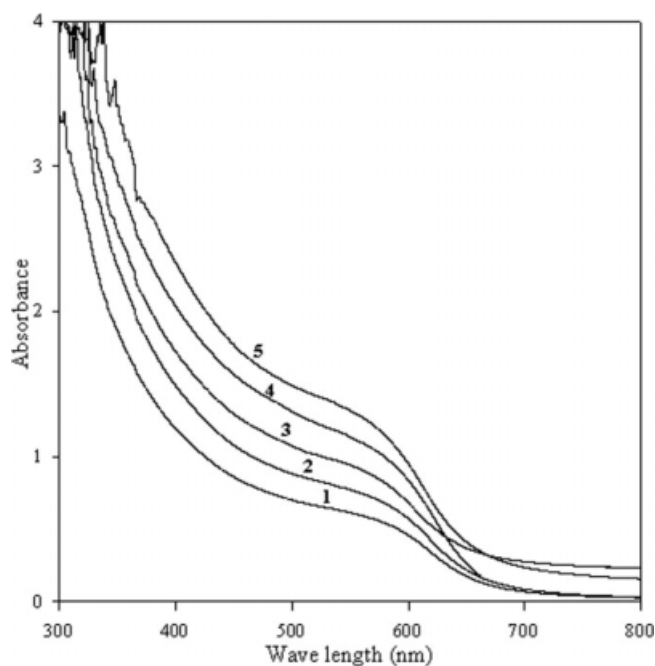


**Figure 3** UV-visible spectra of the samples in water at 6 wt % concentration.

condition  $\lambda < \lambda_c$  is applicable, where  $\lambda_c$  is linearly proportional to the interparticle distance ( $d$ ).<sup>19</sup> By correlating our results with those of previous studies, we conclude that the colors of our samples must

have resulted from the selective Bragg diffraction of visible light at  $\lambda < \lambda_c$ .

#### Laser light scattering studies of P(NIPAAm-HEAc)/ $\beta$ -CD particles

Figure 4 shows the DLS spectra of Samples 1, 3, and 5 at 25°C and at a temperature above the LCST. The microgels are in their swollen state and have a narrow size distribution except for Sample 5. The average diameters of Samples 1, 2, 3, 4, and 5 were 179, 200, 237, 313, and 568 nm at 25°C and 67, 72, 80, 99, and 129 nm when heated above their LCST, respectively. The LSS studies of the nanoparticles showed an increase in their average radii after the incorporation of  $\beta$ -CD at temperatures below the phase transition temperature. As a result of the incorporation of  $\beta$ -CD, the particle size increases, whereas the microgels show a narrow size distribution, which demonstrates the formation of a homo inclusion complex.<sup>34</sup> When the amount of CD is increased beyond 40%, a broad distribution of the radius was seen, indicating the aggregation of the nanoparticles arising from the enhanced  $-\text{OH}$  interactions. When the temperature was increased above the LCST, the microgels shrank sharply with a narrower size distribution but were found to be fully dispersed throughout the solvent. The NIPAAm microgel can act as a water reservoir

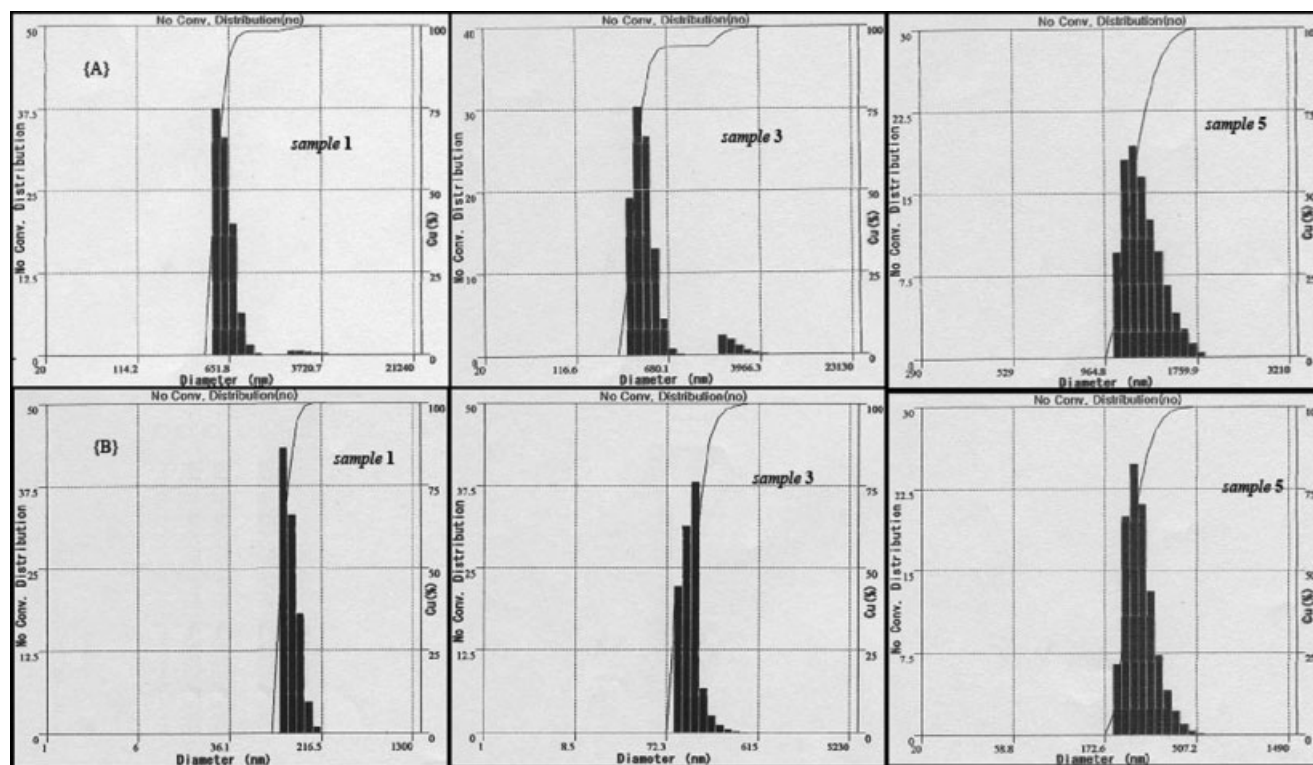


**Figure 4** Hydrodynamic radius distribution of (A) hydrogel nanoparticles at 25°C, (B) hydrogel nanoparticles at temperatures above the LCST, i.e., 40°C (Sample 1), 50°C (Sample 3), and 60°C (Sample 5) measured in water using the dynamic light scattering method.

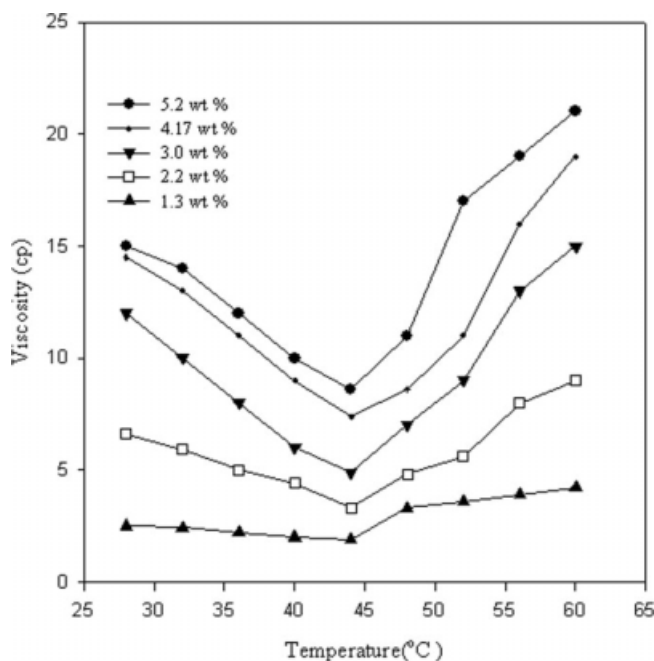


**Figure 5** Temperature-dependent viscosities of aqueous dispersions of Sample 3 inclusion complexes at different polymer concentrations.

because it can shrink very quickly and expel water from the gel efficiently on heating. On heating, the shrinkage of the pendent segments on the microgel particle surface, which are not as dense as the central network,<sup>35</sup> will make the particles more uniform and cause the particle size to be more narrowly distributed.

### Temperature-induced phase transitions

The temperature-induced phase transitions were also evaluated using the viscosity changes and optical properties of the aqueous dispersions. A Brookfield viscometer with a shear rate of 100 rpm gave the viscosity ( $\eta$ ) as the ratio of the shear stress ( $\tau$ ) to the shear rate  $\dot{\gamma}$ . The viscosities of the dispersion of Sample 3 in the range of concentrations from 5.2 to 1.3 wt % at a heating rate of 2°C/5 min are given in Figure 5. The viscosities of all of the samples decreased continuously with increasing temperature up to the LCST, which can be attributed to the shrinkage of the nanoparticles.<sup>36</sup> As the temperature increased beyond the critical point, the viscosities began to increase again after a distinct minimum marking the LCST of the samples. This clear shear thinning of the dispersion at temperatures above the critical temperature is consistent with the formation of a network through the weak associations of hydrophobic interactions.<sup>37</sup> At a lower wt % (>2 wt %) of the polymers in water, the viscosity increased without gelling and, at higher concentrations (<5 wt %), a drastic increase of the viscosity beyond the mea-

surement ranges was observed, due to the gelation caused by the attractive interaction between the nanoparticles. The minimum viscosities of Samples 1, 2, 3, 4, and 5 at a polymer concentration of 3 wt % were 6.52, 5.45, 4.9, 3.46, and 2.1 cP at temperatures of 33, 39, 44, 52, and 57°C, respectively. This result clearly indicates that the LCST of the complex is shifted to higher temperatures as a result of the cyclodextrin inclusion.

The optical properties in relation to temperature were also utilized to estimate the transition temperature of the synthesized particles. The hydrogels exhibit a shoulder-shaped curve corresponding to the color below their critical temperature. This shoulder diminishes as the temperature is raised and disappears above the LCST [Fig. 6(A)]. The inclusion of the nanoparticles also endows the hydrogels with remarkable thermal stability. The iridescent pattern at room temperature became invisible when Samples 1, 2, 3, 4, and 5 were heated above 33, 39, 44, 52, and 57°C, respectively, at which point the color of the gel disappeared and they became cloudy due to phase separation, which is evident from the opacity of the system, as shown in Figure 6(B).

### Drug delivery studies of P(NIPAAm-HEAc)/ $\beta$ -CD hydrogels

The drug release kinetics from the synthesized particles was studied using 5-FU as the model drug. The UV-visible spectra of different amounts of 5-FU (1–7 mg) dissolved in 10 mL of buffer solution at 27°C were taken and the calibration curve was drawn by plotting the absorbance maxima, obtained from the UV-visible spectra, along the Y-axis and the concentration of 5-FU along the X-axis (Fig. 7). To investigate the amount of drug absorbed, perfectly dried samples were immersed in a known concentration of 5-FU solution in pH 7 buffer solutions at 27°C. The UV-visible spectra of the solutions were taken at regular intervals to monitor the amount of drug uploaded, until the saturation point was reached.

The amount of drug incorporated inside the polymers was obtained from the calibration curve by extrapolating the absorbance maxima to the concentration axis and, finally, the loading capacity (LC) was calculated using eq. (1). We observed that  $\sim$  45% of 5-FU in the solution was incorporated into the hydrogel matrix within 24 h (Table II).

To evaluate the amount of drug released, the samples loaded with 5-FU were transferred to pH 7 buffer solutions at different temperatures and the UV-visible spectra of the solutions were monitored after regular intervals of time. The amount of drug released was estimated from the calibration curve. The cumulative release of 5-FU from the samples at

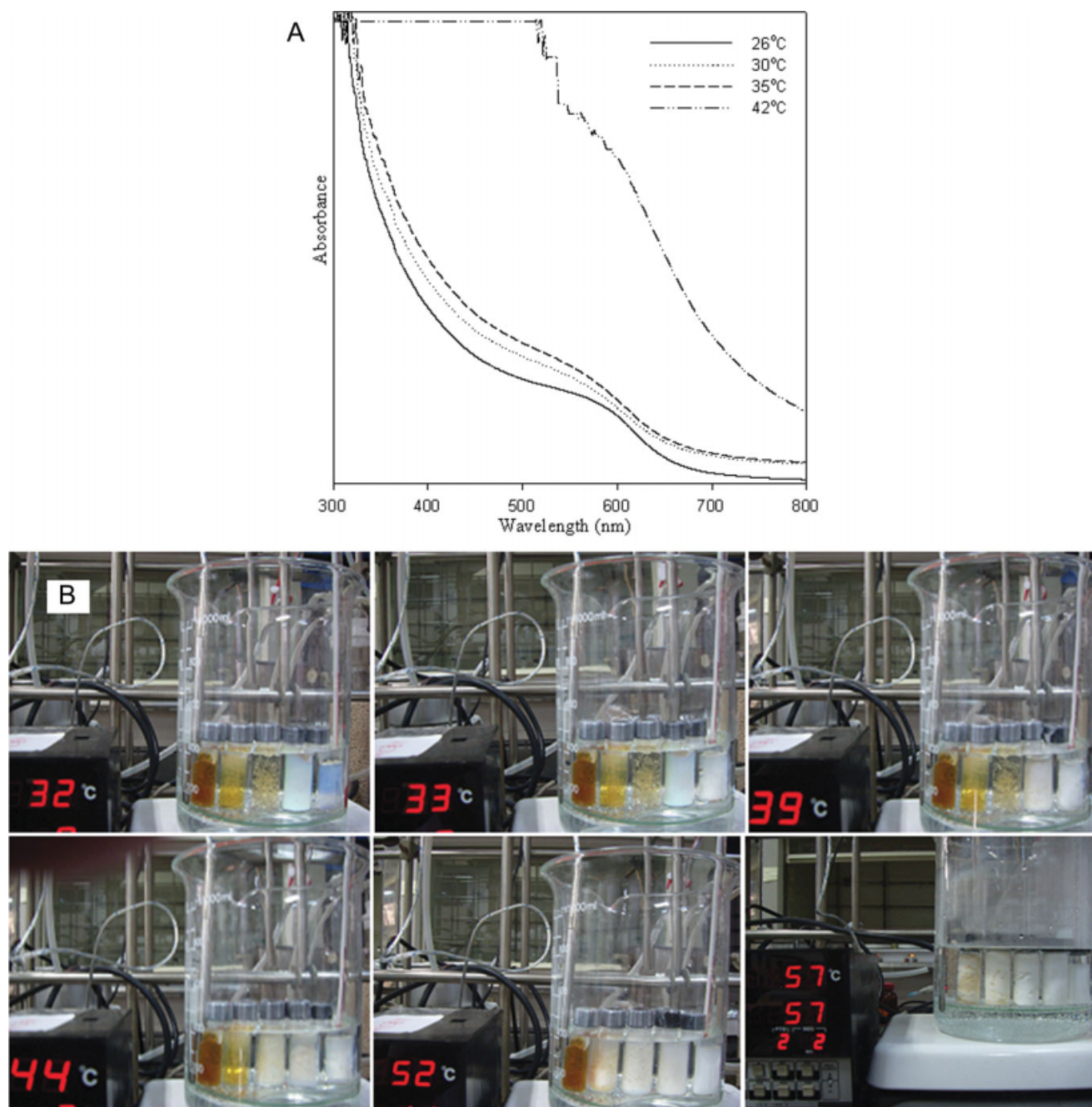


**Figure 6** The phase behavior of the synthesized particles: (A) UV-visible spectra of 4.99 wt % of Sample 2 at different temperatures. (B) Photographs of Samples 1, 2, 3, 4, and 5 (right to left) at 3.0 wt % showing their appearances at 32, 33, 39, 44, 52, and 57°C, respectively. [Color figure can be viewed in the online issue, which is available at [www.interscience.wiley.com](http://www.interscience.wiley.com).]

25 and 37°C as a function of time is given in Figure 8. For Sample 1 without any CD, the hydrogel exhibited an initial burst release of 5-FU and around 50% of the total amount of the drug was found to be released within the first 30 min, with the maximum saturated release (96%) occurring within 6 h. On the other hand, Samples 2, 3, and 4 containing CD showed a slow release, with around 50% release occurring within the first 2–3 h and a maximum release of 90–95% within 10–11 h. In the case of

Sample 5, the amount of drug loaded was very low and the release profile also unexpectedly showed an initial burst. The reason for the observed phenomena can be described as follows: Generally, drug release from a gel is controlled by two factors: (1) the diffusivity of the drug and (2) the swelling of the polymer. When a gel is placed into a solution at constant temperature and pH, water molecules begin to diffuse through the gel surface and enter the medium. At the same time, the drug molecules start to diffuse

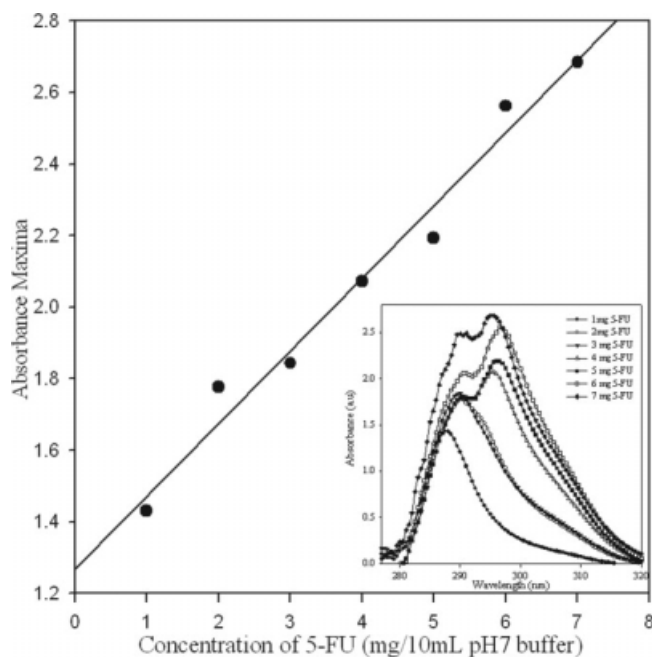


**Figure 7** Calibration curves of 1.0–7.0 mg of 5-fluorouracil, in 10 mL pH 7 buffer solution. The insets shows the UV-visible spectra of 1.0–7.0 mg of 5-FU in pH 7 buffer solution.

through the gel surface and enter the medium. Thus, the first burst release is probably due to the fast diffusion of the drug accumulated on the surface during the process of loading.<sup>9</sup> In the case of the inclusion complexes, the release mechanism is more complicated, owing to the intricate interactions. It has been reported that 5-FU, as a hydrophilic drug,<sup>38</sup> will be trapped within the pores between the polymer chains. When the CD encapsulating the hydrogel reswelled, the 5-FU in the voids of the network first diffused out slowly, resulting in a controlled release. The unexpected low loading and initial burst rate for Sample 5 can be attributed to the enhanced –OH interactions of the polymer network due to excess CD content, which results in the accumulation of drug molecules in the gel surface without entering the network. The release rate

decreases with increasing temperature, due to the aggregation of the polymer chains occurring as a result of the hydrophobic interaction driving force among the hydrophobic groups.<sup>39</sup> Sample 1 was found to release 89% of the drug incorporated into its matrix at 37°C. The inclusion complexes at 37°C showed almost the same release rate below their LCSTs, due to the stability imparted by the inclusion inside  $\beta$ -CD.

## DISCUSSION

The encapsulation of drugs in different host systems serves as an effective tool for drug targeting, which in turn increases the therapeutic efficacy and reduces the side effects associated with the drugs.<sup>29</sup> Among the numerous carriers employed for stable and protective drug delivery, nanotechnology offers the most unique and intriguing approach in the area of nanomedicine.<sup>26</sup> In an attempt to formulate a temperature sensitive carrier system for controlled release, P(NIPAAm-HEAc) hydrogel nanoparticles were developed. The resulting nanoparticles exhibited a spontaneous response to stimuli, but were unstable. In our previous publication, the P(NIPAAm-HEAc) nanoparticles were stabilized by the covalent bonding of the nanoparticles and the drug release rate was studied.<sup>9</sup> The inclusion of the nanoparticles inside cyclodextrin cavities helps to improve the biocompatibility together with the stability of the particles. The hydrodynamic radii of the particles were also found to increase, resulting in the shift of the peaks in the UV-visible spectra to higher wavelengths. The incorporation also enhanced the LCST of the resulting particles compared with the covalently bonded particles examined in our previous study. We were able to tailor the LCST of the colloidal crystals thus formed. The burst release of 5-FU, as observed in our previous study, was changed to slow delivery by the incorporation of the drug into the CD cavities. Being a hydrophilic drug, 5-FU penetrates into the space between the polymer chains, which results in slow delivery, whereas a

**TABLE II**  
Amount of 5-FU Incorporated in P(NIPAAm-HEAc)/ $\beta$ -CD Complexes

Sample	$C_0$ (mg)	$A_{0(\max)}$	$A_{24(\max)}$	$C_{24}$ (mg)	$W_d$ (mg)	Drug loaded (%)
1	5	2.19	1.79	2.6	2.4	48
2	5	2.19	1.81	2.7	2.3	46
3	5	2.19	1.83	2.7	2.3	46
4	5	2.19	1.78	2.6	2.4	48
5	5	2.19	1.84	2.8	2.2	44

$C_0$  = Initial amount of fluorouracil in pH 7 buffer solution (5 mg/10 mL);  $A_{0(\max)}$  = Absorbance maxima corresponding  $C_0$ ;  $A_{24(\max)}$  = Absorbance maxima after immersing hydrogel opal for 24 h;  $C_{24}$  = Amount of fluorouracil corresponding to  $A_{24(\max)}$ ;  $W_d$  = Amount of drug incorporated in samples.



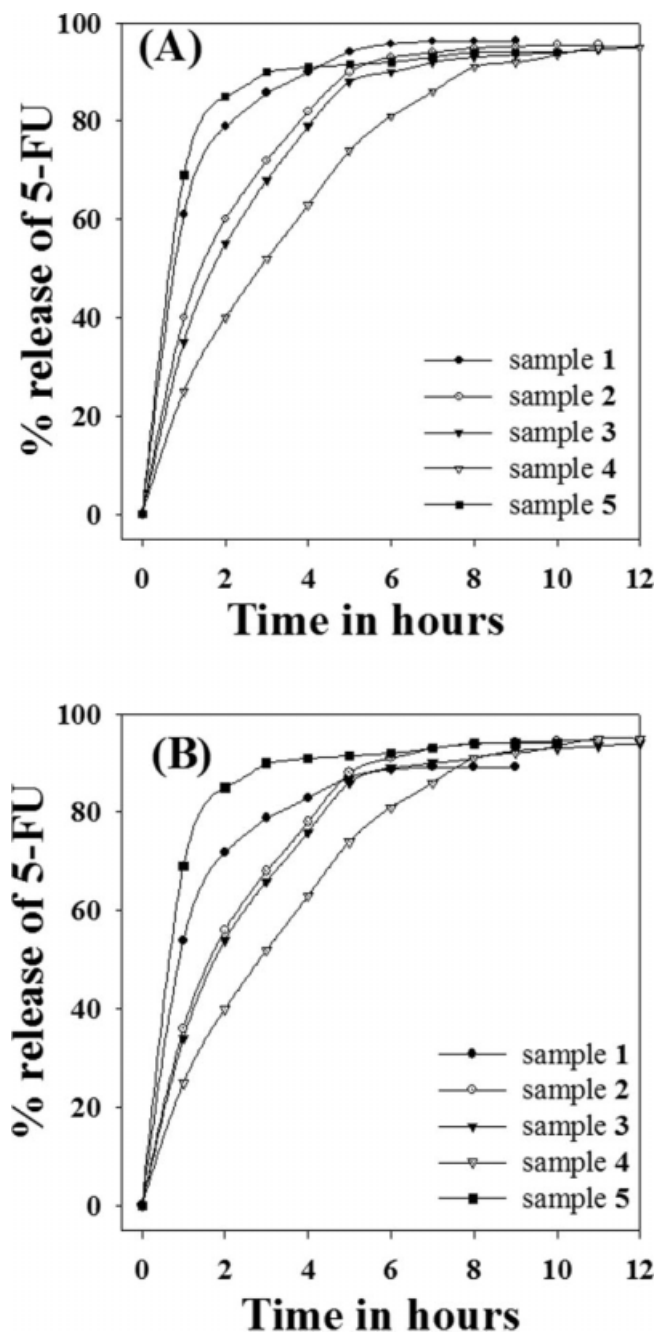


**Figure 8** Cumulative release of 5-FU from P(NIPAAm-HEAc) and P(NIPAAm-HEAc)/ $\beta$ -CD hydrogels at (A) 25°C and (B) 37°C.

burst release profile was observed in our previous study.<sup>9</sup> The inclusion complexes also showed higher release at 37°C in pH 7 solutions when compared with the P(NIPAAm-HEAc) nanoparticles stabilized by covalent bonding in our previous study.<sup>9</sup> This is due to the enhancement of the LCSTs as a result of the CD inclusion, which can be varied by adjusting the CD concentration. This approach would be appropriate for the delivery of various drugs, both hydrophilic and hydrophobic, (which will be our future focus) and could find potential applications.

## CONCLUSIONS

Novel supramolecular inclusion complexes of poly[*N*-isopropylacrylamide-*co*-2-hydroxyethylacrylate] nanoparticles in varying amounts of  $\beta$ -cyclodextrin, whose self-assembly led to the formation of colloidal crystals, were successfully synthesized. The hydrodynamic radius of the particles increased as the amount of  $\beta$ -CD increased, and this was accompanied by the enhancement of the lower critical solution temperature up to 55°C. The improved biocompatibility, water solubility, and stability imparted to these complexes by the cyclodextrin moieties favors their application as a good drug delivery system. Our study showed that the incorporation of CD results in the slow release of 5-FU from the gel, which can be attributed to the formation of host-guest interactions between the drug molecules and cyclodextrin groups.

## References

- Freitas, R. F. S.; Cussler, E. L. *Chem Eng Sci* 1987, 42, 97.
- Chen, G.; Hoffman, A. S. *Nature* 1995, 373, 49.
- Tanaka, T.; Nishio, I.; Sun, S. T.; Ueno-Nishio, S. *Science* 1982, 218, 467.
- Im, S. J.; Choi, Y. M.; Subramanyam, E.; Huh, K. M.; Park, K. *Macromol Res* 2007, 15, 363.
- Kopeček, J. *Nature* 2002, 417, 388.
- Monji, N.; Hoffman, A. S. *Appl Biochem Biotechnol* 1987, 14, 107.
- Peppas, N. A.; Bures, P.; Leobandung, W.; Ichikawa, H. *Eur J Pharm Biopharm* 2000, 50, 27.
- Bae, Y. H.; Okano, T.; Kim, S. W. *Makromol Chem Rapid Commun* 1988, 9, 185.
- Mathews, A. S.; Ha, C.-S.; Kim, I. *Drug Deliv* 2006, 13, 245.
- Son, Y. K.; Kim, J. H.; Jeon, Y. S.; Chung, D. J. *Macromol Res* 2007, 15, 527.
- Kawaguchi, H.; Fujimoto, K.; Mizuhara, Y. *Colloid Polym Sci* 1992, 270, 53.
- Ritter, H.; Sadowski, O.; Elmar, T. *Angew Chem Int Ed Engl* 2003, 42, 3171.
- Winnik, F. M.; Ottaviani, M. T.; Turro, N. J. *Macromolecules* 1991, 25, 6007.
- Louai, A.; Sarazin, D.; Francois, J. *Polymer* 1991, 32, 713.
- Wu, X. J.; Peltron, R. H.; Tam, K. C.; Woods, D. R.; Hamielec, A. E. *J Polym Sci Part A: Polym Chem* 1993, 31, 957.
- Bae, Y. H.; Okano, T.; Kim, S. W. *Pharm Res* 1991, 8, 531.
- Qiu, Y.; Park, K. *Adv Drug Delivery Rev* 2001, 53, 321.
- Kabra, B. G.; Gehrke, S. H.; Spontak, R. J. *Macromolecules* 1998, 31, 2166.
- Hu, Z. B.; Gao, J. *Adv Mater* 2001, 13, 1708.
- Forming, K. H.; Szejtli, J. *Topics in Inclusion Science*; Kluwer Academic Publishers: Boston, MA, 1994.
- Harada, A.; Li, J.; Kamachi, M. *Nature* 1993, 364, 516.
- Lo Nostro, P.; Lopes, J. R.; Ninham, B. W.; Baglioni, P. *J Phys Chem B* 2002, 106, 2166.
- Xiao, J. B.; Chen, X. Q.; Yu, H. Z.; Xu, M. *Macromol Res* 2006, 14, 442.
- Won, J.; Yoo, J. Y.; Kang, M. S.; Kang, Y. S. *Macromol Res* 2006, 14, 449.
- Smay, J. E.; Cesarano, J. J.; Lewis, A. *Langmuir* 2002, 18, 5429.
- Ha, D.; Lee, S. B.; Chong, M. S.; Lee, Y. M. *Macromol Res* 2006, 14, 87.

27. Park, J. S.; Han, T. H.; Lee, K. Y.; Han, S. S.; Hwang, J. J.; Moon, D. H.; Kim, S. Y.; Cho, Y. W. *J Controlled Release* 2006, 115, 37.
28. Stella, V. J.; Rajewski, R. A. *Pharm Res* 1997, 14, 556.
29. Banerjee, R.; Chakroborty, H.; Sarker, M. *Biopolymers* 2004, 75, 355.
30. Han, S. J.; Yoo, M. K.; Sung, Y. K.; Lee, Y. M.; Cho, C. S. *Macromol Rapid Commun* 1998, 19, 403.
31. Hu, Z.; Lu, X.; Gao, J.; Wang, C. *Adv Mater* 2000, 16, 1173.
32. Hu, Z.; Lu, X.; Gao, J.; Cai, T.; Huang, G.; Zhou, B. U.S. Pat. 0018160A1 (2004).
33. Jethmalani, J. M.; Ford, W. T.; Beaucage, G. *Langmuir* 1997, 13, 3338.
34. Xia, X.; Hu, Z. *Langmuir* 2004, 20, 2094.
35. Gao, J.; Hu, Z. *Langmuir* 2002, 18, 1360.
36. Xia, X.; Hu, Z.; Marquez, M. *J Controlled Release* 2005, 103, 21.
37. Durand, A.; Hourdet, D. *Polymer* 1999, 40, 4941.
38. Nounou, M. M.; El-Khordagui, L. K.; Khalafallah, N. A.; Khalil, S. A. *Acta Pharm* 2006, 56, 311.
39. Zhang, J. T.; Huang, S. W.; Cheng, S. X.; Zhuo, R. X. *J Polym Sci Part A: Polym Chem* 2004, 42, 1249.